Posted: December 9, 2025

A Textile High Impedance Surface Designed for High Yield Manufacturing

S. Henthorn[1,*], W. Hurley[2], and A. Tennant[1]

[1]School of Electrical and Electronic Engineering, University of Sheffield, Sheffield, UK
[2]ottingham School of Art and Design, Nottingham Trent University, Nottingham, UK
[*]Corresponding author: s.henthorn@sheffield.ac.uk

Abstract

A textile high impedance surface (HIS) with low production time and broad surface wave suppression bandwidth is designed, modeled as an isotropic and anisotropic structure, fabricated and measured. Textile HIS are well suited to mitigating surface wave propagation across conformal parts on an aircraft due to their flexibility, high strength and low weight, and they have previously been produced using computerized flat-bed knitting. However, fabricating the large surface areas of material required in practical timescales has been a challenge, particularly when complex techniques such as integrated vias are utilized. Here, through co-design of electromagnetic performance and efficient weft knitting production methodologies, a high-yield method to produce a petal-like design is presented and characterized. Production times are reduced by a factor of 20 compared with previous designs. Anisotropic electromagnetic performance is measured and modeled in the weft knitted HIS. The fabricated design is able to suppress surface wave transmission by more than 10dB in the band between 9 and 15 GHz.

1 INTRODUCTION

High impedance surfaces (HIS), also known as electromagnetic band-gap (EBG) materials or artificial magnetic conductors (AMCs), are well established metamaterials for radar cross section (RCS) reduction and antenna enhancement. They suppress the transmission of surface waves over a given frequency range, and provide 0^o phase shift on reflection. This makes them useful for reducing the contribution of creeping waves to an object's RCS, and for isolating antennas from the surrounding environment such as metallic ground planes Sievenpiper (1999). Conventionally, these would be made with PCB etching techniques on rigid substrates.

HIS integrated into the body of an aircraft would offer significant advantages, such as suppression of creeping waves which contribute to the platform's RCS. They can also prevent crosstalk between antenna arrays and allow near-planar antennas to be fitted to the platform, reducing aerodynamic drag from communications equipment significantly. However, to achieve these aims the HIS must be conformal to the shape of the aircraft rather than flat and rigid.

Textile HIS provide a solution to this, with attractive features including high levels of conformability to complex surfaces, while still having low weight and high strength. Certain techniques, such as weaving and knitting, also have the advantage of utilizing existing commercial processes, such as looms and knitting machines, to cheaply produce large-area metamaterials at low cost.

Several approaches to the production of textile metasurfaces have been developed Ferreira et al. (2018), from the initial use of copper tape on a felt substrate Salonen et al. (2004), through screen or inkjet printing on woven fabrics Seager et al. (2013); Whittow et al. (2014), to designs embroidered using conductive threads Baum et al. (2016). The most common approach for HIS designs in recent years has utilized premade conductive fabrics and sewn them onto non-conductive fabric substrates, including felt and denim Shamsuri Agus et al. (2022); Ashyap et al. (2021a).

One key disadvantage of the above approaches is that none allows the use of vias between the resonant element and the ground plane Ali et al. (2023); Keshwani and Rathod (2022). These are often used to improve the performance of HIS, such as in the classic "mushroom" surface design Sievenpiper (1999). Some have simulated performance with designs which include vias, but experimental results are not presented

Wajid et al. (2022). To overcome this while maintaining performance, significantly more complex element designs can be used, at the cost of increasing fabrication complexity and production time Ashyap et al. (2021b).

Flatbed machines are the most versatile type of weft knitting machine and are available as hand-operated and automated machines. They are capable of efficiently producing large areas of fabric (over $2m^2$) on a single roll. Industrial flatbed machines typically have two needle beds aligned in an inverted V configuration, which can either knit independently to create single bed fabric (single jersey) or together to create rib (double jersey) fabrics. Selectively knitting on one or both beds allows for a broad range of knitted structures.

Weft knitting has been proposed as a solution to producing HIS with integrated vias in a single continuous process Tennant et al. (2013). A conductive yarn was used for the ground plane and surface pattern elements, with non-conductive polyester yarn as the spacing substrate. Vias are created by knitting the yarn between the top layer and the ground plane, electrically connecting the two at the desired locations. The element shapes used were bow-tie patches with point vias at the extremities, similar to those conventionally used in HIS due to their ease of simulation and production with PCB etching. However, when translated to flat-bed knitting, while they were able to be fabricated, the production time was significant. During manufacture, each segment of the bow-tie is knitted individually across the width of the fabric with vias at each corner. This manufacturing methodology requires multiple movements of the yarn feed, repeated across the width of the knitted fabric, for each triangular section of the bow-tie. Therefore, each knitted row could have several hundred time consuming yarn carrier movements. This significantly limits its usefulness for producing large-area metasurfaces for aerospace applications.

This paper aims to overcome this by utilizing a new knitting method with two yarn carrier feeds, which separate to knit the surface pattern and combine to knit the rear ground plane. The manufacturing process means there is a via between ground and element whenever the unit cell design moves from insulating material to conductive material. This opens up opportunity for co-design of a new HIS element which can achieve good suppression of surface waves in the 9-16 GHz band, while being easily produced at scale using flat-bed knitting. This work seeks to address important questions in how metasurfaces can be manufactured at scale, and how to model the performance of textile metasurfaces accurately and efficiently.

In Section 2, the knitting procedure is introduced, and its influence on electromagnetic design discussed. The process of designing the new HIS element is presented in Section 3, including simulation of the unit cell geometry assuming isotropic conductivity of the knitted fabric. The effect of anisotropy is investigated in Section 4 through further modeling. Section 5 then discusses the fabrication and measurement of the HIS reflectivity and its performance in suppressing surface waves. Lessons learned from the modeling process are discussed in Section 6, before conclusions are drawn in 7.

2 KNITTING PROCEDURE AND INFLUENCE ON DESIGN

The desired metasurface structure consists of a continuous conductive ground plane and a conductive pattern of unit cells, separated by an insulating spacer layer but with interconnecting conductive vias between the ground and pattern. To achieve this, a knitting method is proposed with two yarn carrier feeds of the same type of conductive yarn combining to knit the ground plane on the rear needle bed. Where the metasurface pattern appears on the front of the fabric the conductive yarn carriers will separate with one knitting the ground plane on the rear needle bed and one knitting the metasurface element on the front needle bed. The separation of the carriers between ground plane and the metasurface pattern leads to the creation of a via connection. The surface pattern layer is a combination of conductive and non-conductive (polyester) elements.

A polyester spacer yarn is then laid between the pattern layer and the ground plane to ensure connection only occurs at the vias. This method drastically reduces the number of yarn movements for multiple surface pattern elements which in turn reduces manufacturing times considerably. Due to the manufacturing method a via is created where the pattern along each linear course transitions between non-conductive and conductive pattern.

The method also presents interesting and novel design considerations and opportunities. The most significant is that vias must be placed around the edges of conductive patches, rather than in the middle as in the classic "mushroom" design Sievenpiper (1999). The distance between the knit also has an influence,

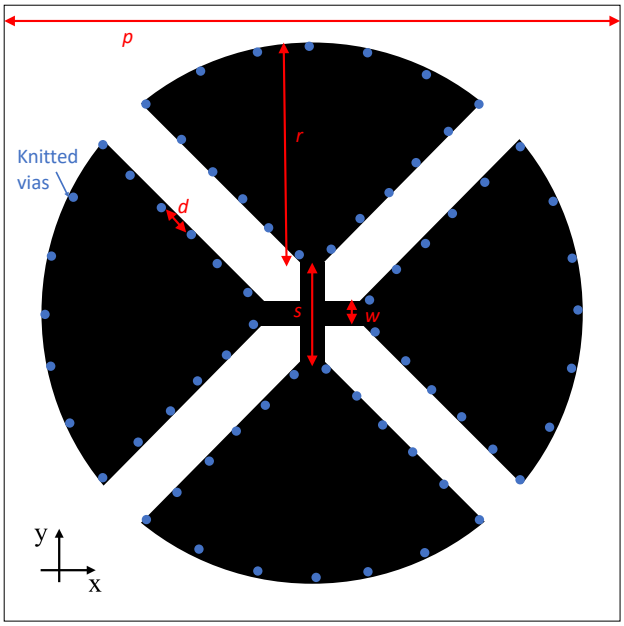

Figure 1: Schematic of designed HIS unit cell

with a smaller knit producing more vias than a larger knit. The effects of these on electromagnetic performance are investigated in the following section. It should also be noted that the spacer does not maintain a constant distance between the continuous ground plane and the patches, as it contracts at the site of the vias due to the cross-knit between them.

3 DESIGN AND MODELING OF KNITTED HIS

The aim of the design process is to produce an HIS capable of wideband suppression of surface waves in approximately the range 9 GHz to 15 GHz. This will be achieved by positioning an initial resonance at around 8 GHz to define the onset of surface wave suppression, then further higher-order resonances up to 15 GHz spaced out evenly to maintain suppression across the frequency band. This will be done through simulation of the reflectivity of the surface, examining the location of resonances which cause the reflected phase to pass through 0^o.

The general element design is shown in Fig. 1. It is similar to a conventional cross element, but with expanded and curved fans to each arm to increase the bandwidth of operation. The element can be approximated as a circle with radius r mm, which has been quartered and separated by s mm. The quarter circles are connected by a cross with arms of length s mm and width w mm. Vias are knitted around the edges of the quarter circles to control higher-order resonances, separated by knit distance d. The pattern repeats with period p mm, and the main thickness of the spacer is t mm. The materials chosen for the work were Shieldex 235/6 as the conductive thread, which is a silver-plated 235 Denier filament polaymide 6.6 yarn; and polyester as the spacer material.

In order to investigate the element's behavior and produce a final design, a simplified version was simulated using Floquet Mode boundaries in CST Microwave Studio. The polyester spacer was modeled as a rectangular sheet of thickness 4 mm, with relative permittivity 4.2 and loss tangent 0.0002 Liu et al. (2019). The vias were modeled as cylinders of 0.5 mm diameter, passing vertically through the polyester to the continuous ground plane. Conductive areas were modeled as infinitely thin sheets with conductivity $\sigma = 10^5$ S/m in all directions. This surface impedance approach is a major simplification for a lossy conductor, but reduces the computational load of simulation to a level where design can be carried out. The effects of this simplification will be explored in Section 4.

Simulated reflectivity performance as key parameters are varied are shown in Fig. 2 and Fig. 3. When not being varied, the values are held as in Table 1. Variation of both s and w were found to have minimal effect on the resonant behavior of the HIS, so are not included in detail in simulation results.

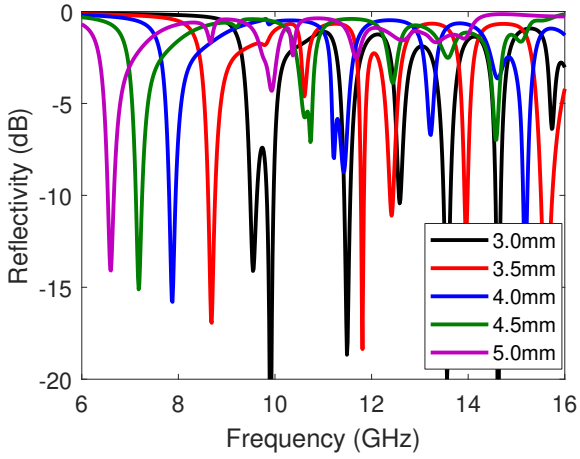

(a)

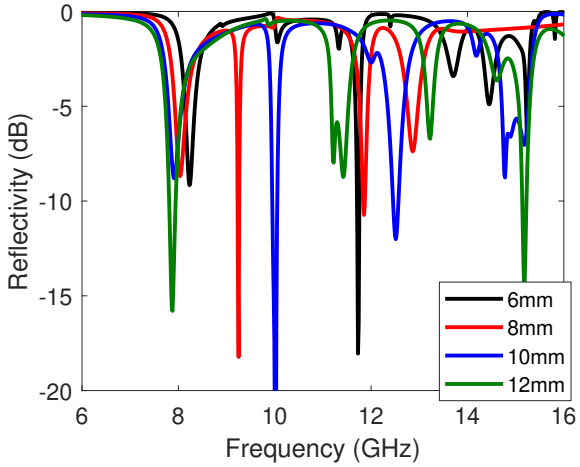

(b)

Figure 2: Simulated knitted HIS, varying (a) Substrate thickness t, (b) quarter circle radius r

As with all HIS, the main resonance is most heavily dependent on the thickness of the substrate between the patch and the ground, t, and the size of the resonant patch, here most closely matched to r. Increasing t leads to a lower primary resonance, and also brings the secondary resonances down as well. Increasing r, meanwhile, leads to a slight decrease in the primary resonance, but a significant shift down in frequency of the secondary and tertiary resonances. Similarly, altering p has little influence on the fundamental resonant frequency but shifts the higher frequency resonances lower as p increases. As such, p should be chosen to be as small as possible for a given r and s to maximize spacing between the resonances, giving as broadband behavior as possible.

Varying d, and so both the number of and distance between the vias, introduces more subtle effects. When the vias are closely spaced (d=1-2 mm), there is little change in behavior. However, as the vias become sparser, the fundamental resonance begins to come lower and new resonances emerge between 8 and 10 GHz. Note however that the former secondary resonance at 11.5 GHz seems to remain near constant

Table 1: Dimensions of unit cell design

Parameter	Dimension (mm)
t	4
r	12
p	33
d	2
s	5
w	1

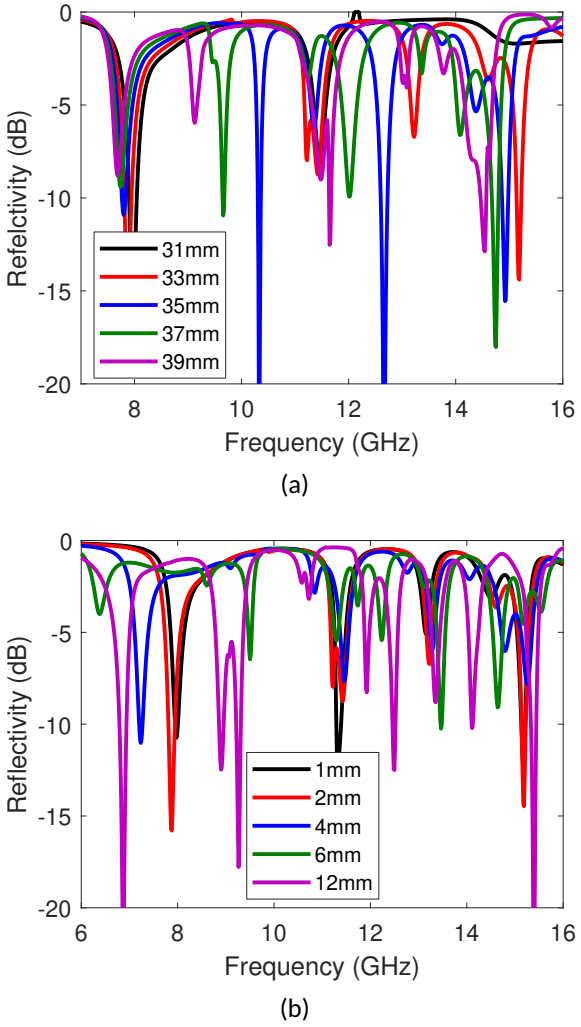

Figure 3: Simulated knitted HIS, varying (a) element periodicity p, and (b) knit spacing between vias d

as the knit changes. As such, the closely spaced vias maintain the desired single deep resonance at round 8 GHz, followed by higher order resonances at around 12 GHz.

The final design uses the dimensions described in Table 1, with simulated reflection characteristics in Fig. 4. In order to achieve good suppression of surface waves between 9 GHz and 15 GHz, the first resonance, and so the 3dB suppression point for surface waves, is designed to appear at 8 GHz. As such, by 9 GHz the suppression should be significantly greater. The next resonances are spaced as evenly as possible, at 11 GHz, 13 GHz and 15 GHz, to try and maintain broadband suppression across this bandwidth.

To further examine the behavior, the surface currents are shown in Fig. 5. At the 8 GHz resonance the whole bow-tie element is resonating, giving the lowest possible resonance. At the higher-order resonances, smaller sections of the element resonate, until at 15 GHz the strongest currents are predominantly between the vias at the center of the patch. This suggests that the higher order resonances are dictated by the placement of the vias, reinforcing the earlier discussion of how varying property d controls these resonances.

4 MODELING ANISOTROPIC BEHAVIOR

The modeling so far assumes that the conductive threads behave as an isotropic sheet impedance. However, previous investigations with embroidered materials have shown that conductive surfaces made of threads with a direction to their knit have different effective conductivities depending on whether the currents run parallel to the threads or perpendicular to them Baum et al. (2016). Weft knitting is different from embroidery, but still has some variation in micro-structure in different dimensions. As can be seen in

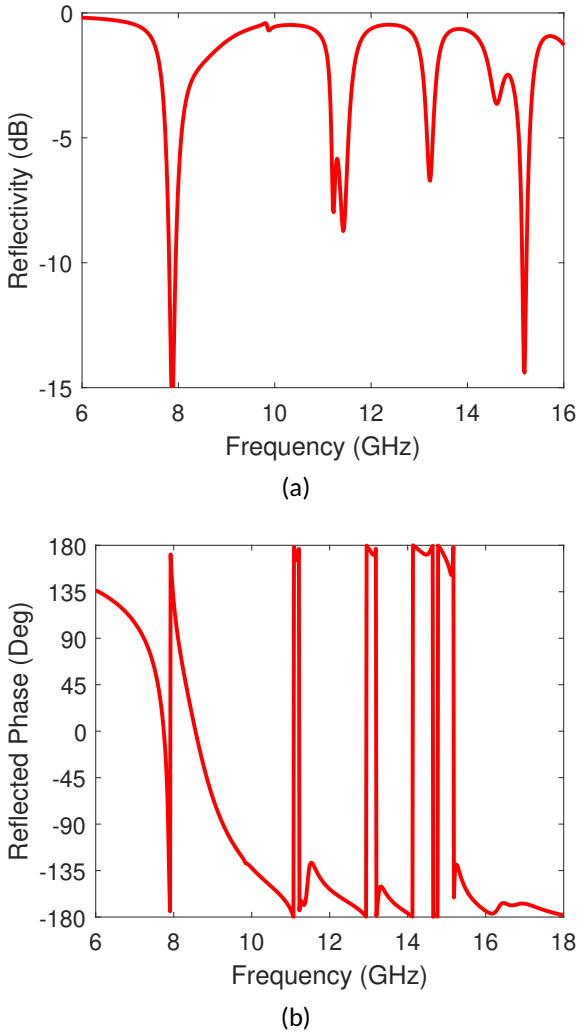

Figure 4: Simulated reflection of final HIS design, (a) Magnitude, (b) Phase

Fig. 6, the loops form continuous lines of contact in the y-dimension (along the wale, in knitting terms). While there is mechanical contact due to the loops in the x-dimension (along the course), this does not appear as a straight line and instead weaves up and down. These contact points are also physically beneath the contact points running in the wale direction. It is well established that this causes mechanical anisotropy Karger-Kocsis et al. (1996), but the effect on conductivity at microwave frequencies is unknown. This section will explore the impact a highly anisotropic conductivity of the knitted conductor would have on electromagnetic performance.

To analyze this, the material was modeled again in CST with the conducting surface material as 0.5 mm thick lossy metal with constant conductivities $\sigma_y = \sigma_z = 10^5$ in the y and z dimensions, while varying the conductivity in the x dimension σ_x. The rest of the geometry and material parameters remained identical. Note the lossy metal model was not used during the design process due to the large computational resource required to model lossy metals compared with surface impedances.

The simulated S11 for the two orientations of incident electric field are shown in Fig. 7. First, there are some slight differences between the isotropic thick lossy metal model and the previous impedance sheet model (Fig. 4), with a reduction in the depth of the primary resonance from around -15dB to -4dB. However, the location of the resonances in frequency are still near-identical between the models.

When anisotropy is introduced, when the incident electric field is aligned with the conductive y dimension the primary resonance still occurs, but is much deeper, reaching -18dB. The overall loss at higher frequencies is also increased to -2dB, and the the 14 GHz resonance no longer occurs. However, when the incident E-field is aligned with the x dimension, the fundamental resonance shifts significantly to 9.5GHz and is a much broader peak. The higher order resonances disappear. Similar results are seen in the reflected phase,

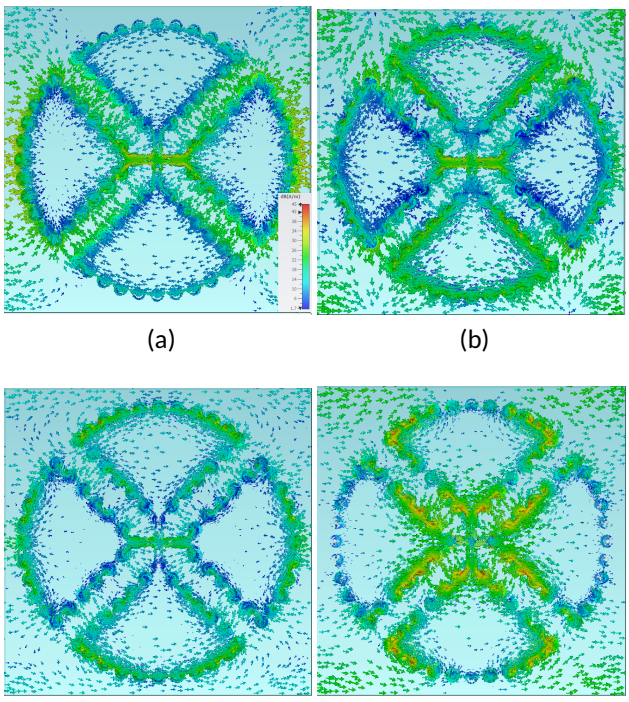

Figure 5: Simulated surface currents on HIS, at resonances (a) 8 GHz, (b) 11 GHz, (c) 13 GHz, and (d) 15 GHz

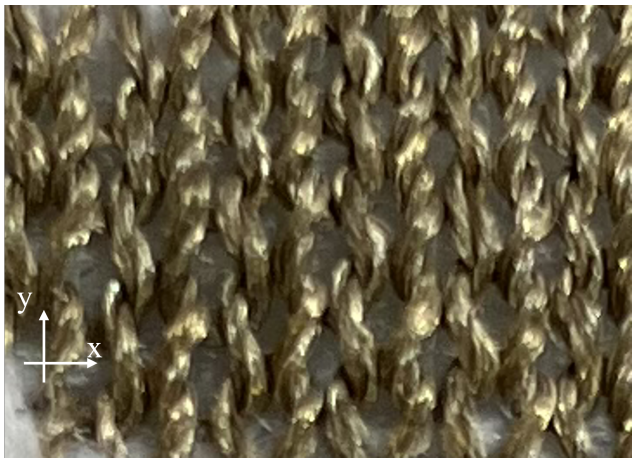

Figure 6: Close-up photograph showing micro-structure of weft knitted material

where the steep crossings through 0^o when the E-field aligns with the conductive dimension of the surface, as seen in the isotropic model, become a single, lower gradient slope in phase when the E-field aligns with the lossy dimension.

Further insight into this behavior is available from observing the surface currents (Fig. 8). At 8 GHz when the E-field aligns with the conductive direction (Fig. 8a), there is a clear resonance across the larger structure, though note the large reduction in current in the central cross of the unit cell in comparison with the isotropic simulation in Fig. 5a. Where the E-field aligns with the non-conductive direction (Fig. 8b), the current distribution across the structure is still present, but with reduced magnitude as this is slightly off the main resonant frequency for this direction.

At the next highest resonance of 11 GHz, where the E-field is aligned with the conductive direction, the currents are strong in the corners of the structure (Fig. 8c). This is again similar to the effect seen in the isotropic model (Fig. 5b). However, when the E-field is in the non-conductive x direction the currents are significantly reduced at these points (Fig. 8d), though there are still some strong currents across the whole

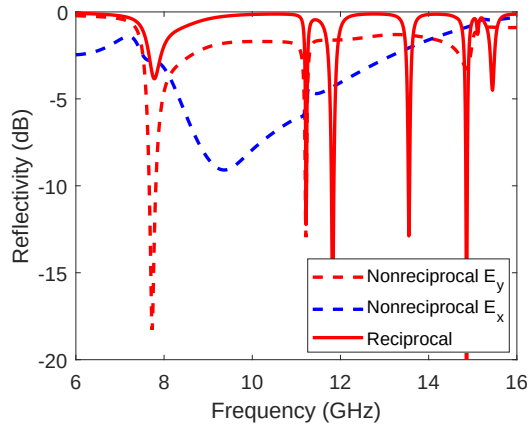

(a)

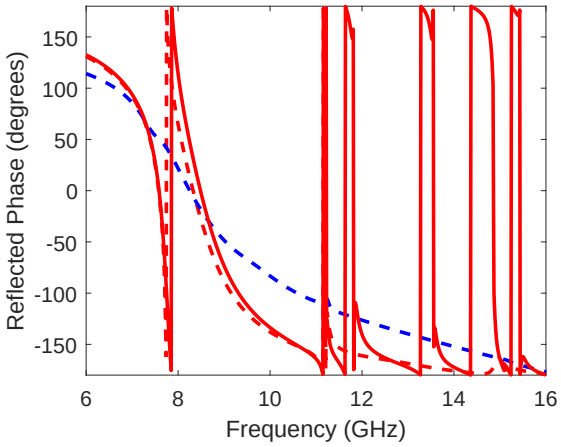

(b)

Figure 7: Simulation of metasurface with anisotropic conductivity $\sigma_x = 10$ S/m and $\sigma_y = \sigma_z = 10^5$ S/m, compared with a isotropic conductivity $\sigma = 10^5$ S/m, (a) Magnitude, (b) Phase

unit cell as the structure is still within its fundamental resonance.

Finally, at the highest resonance of 15 GHz, previously the isotropic model showed strong currents at the center of the unit cell around the vias (Fig. 5d). For the anisotropic model, these currents are still present though reduced for the case with E-field aligned with the conductive y-direction (Fig. 8e). However, when the E-field is aligned with the non-conductive x-direction these currents are not present at all (Fig. 8f). This demonstrates that the higher order resonances around the vias are suppressed by the conductivity being lowered, while the fundamental caused by the whole unit cell structure is still present but shifted in frequency due to the increased loss.

5 FABRICATION AND MEASUREMENT

The fully knitted HIS is shown photographed in Fig. 9. An 8x8 grid of unit cells was produced to ensure a suitably sized sample for measurement. Reflectivity measurements were carried out using an NRL arch at normal angle of incidence.

The measured reflected magnitude and phase of the knitted surface are shown in Fig. 10 for a variety of rotational angles. When the incident E-field is aligned with the y-direction (0^o, or along the wale), the results agree reasonably well with both the isotropic and anisotropic simulated models. All show the primary resonance occurring at 8 GHz, and predict the main higher frequency resonances, though in measured they appear as two deep nulls at 12 GHz and 15 GHz rather than smaller ones at 11 GHz, 13 GHz and 15 GHz. This is likely due to the simplifications made when modeling the structure. First, the fabricated spacer is not a flat

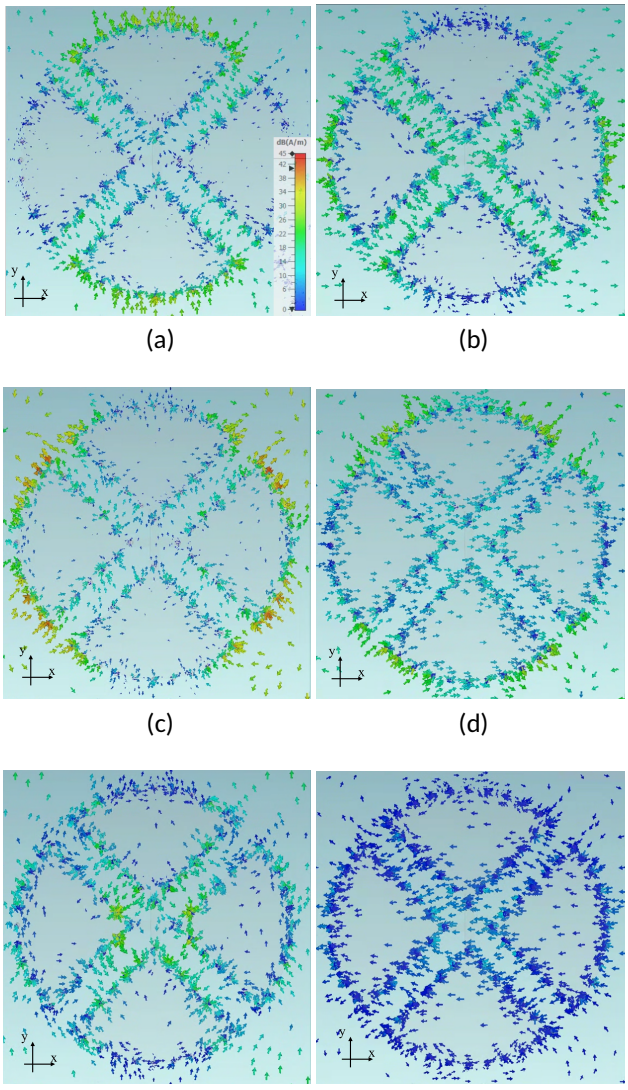

Figure 8: Simulated surface currents on nonreciprocal HIS at (a-b) 8 GHz, (c-d) 11 GHz, and (e-f) 15 GHz when incident wave has E-field in the (high conductivity) y-dimension (a,c,e) or (low conductivity) x-dimension (b,d,f)

rectangle, but instead contracts towards the vias, meaning the spacing varies across the element surface. Second, vias were modeled as vertical cylinders spaced apart by some distance, but when fabricated they are curved and slanted in a continuous knit.

A further difference is the measured resonance at 8 GHz is much deeper than the simulated reflectance, reaching below -30 dB, despite being broader band. This suggests greater loss in the fabricated design, either due to higher resistivity of the threads or loss tangent in the polyester spacer. Despite these discrepancies, the measured surface still shows the expected phase change through 0^o at 8 GHz, demonstrating HIS behavior and that surface wave suppression should begin at this point. The higher order resonance points also show transitions through 0^o reflected phase, suggesting wideband suppression of surface waves should occur. As such, both models have good predictive capacity for designing knitted HIS materials.

As the knitted surface was rotated so the incident E-field is in line with the x-direction (along the course), the performance changes, suggesting that anisotropic conductivity is caused by the weft knit. As predicted with the anisotropic model, the lower resonances shifts to a higher frequency. However, unlike the anisotropic modeled version the deepest resonance occurs at much higher frequency, around 16 GHz, which were predicted not to occur. The explanation for this is likely due to the difference in how the anisotropy is

Figure 9: Photograph of fully knitted HIS

modeled and what causes it in the knitted structure. In the knitted material, conductivity is high along the wales, but is lower when traveling across adjacent threads along the course. This means the anisotropic conductivity model, which assumes conductivity is a function of direction, is good for large-scale structures with many threads, but poor for smaller structures which have only a single thread. The main case in this structure is the areas around the vias, which as discussed in Section 3 control the higher-order resonances. As such, the anisotropic model predicts the fundamental resonance well, but higher-order resonances are better predicted with the isotropic model.

The effect of this anisotropy on surface wave transmission is also investigated. This is measured using the experimental setup described in detail in Cerveny et al. (2023), and shown in Fig. 11. For all rotations, below 7 GHz the surface enhances surface waves, due to acting as a dielectric waveguide at these frequencies. At 0^o rotation the cut-off occurs at around 8 GHz, and continues to beyond the 18 GHz operating frequency of the measurement setup. For 90^o orientation the band is reduced, starting at approximately 10 GHz, in line with the modeled principle resonance in this polarization, but has a similar upper bound. Despite the differences, the textile surface is efficient at suppressing surface waves in both orientations over a broad band of frequencies due to the multiple closely-spaced resonances present in the design.

6 DISCUSSION ON MODELING KNITTED METASURFACES

The investigation in this paper has designed and produced a textile HIS which can be produced at volume. However, the trade-offs with manufacturing have demonstrated the challenges of modeling and designing knitted metasurfaces, but also shows a way forward. For maximum accuracy across the full frequency range, the metasurface should be modeled thread-by-thread to account for the differences between both anisotropic and isotropic models of conductive knitting. However, this is highly computationally expensive, so is unreasonable for design purposes.

The simplest model assumes isotropic performance. This models well the fundamental resonance caused by the large unit cell structure when the E-field aligns with the knit direction, and also the higher order resonant behavior caused by single-thread structures like those around vias. However, they do not predict the performance of the fundamental resonance when the E-field is perpendicular to the knit direction. Anisotropic models are more computationally expensive but do predict the fundamental resonance in both E-field directions, though they do not capture the behavior of the higher order resonances.

As such, the designer of knitted metasurfaces should take into account both isotropic and anisotropic models. They must co-design with the manufacturing process to understand the scale of the knitted microstructure, analyze what behaviors are caused by different macro- and micro-structures, and use these to choose which resonances are predicted by each model. Alternatively, co-design of knit size and element structure could be used to avoid these multiscale problems and target predictable behavior across the range of operating frequencies.

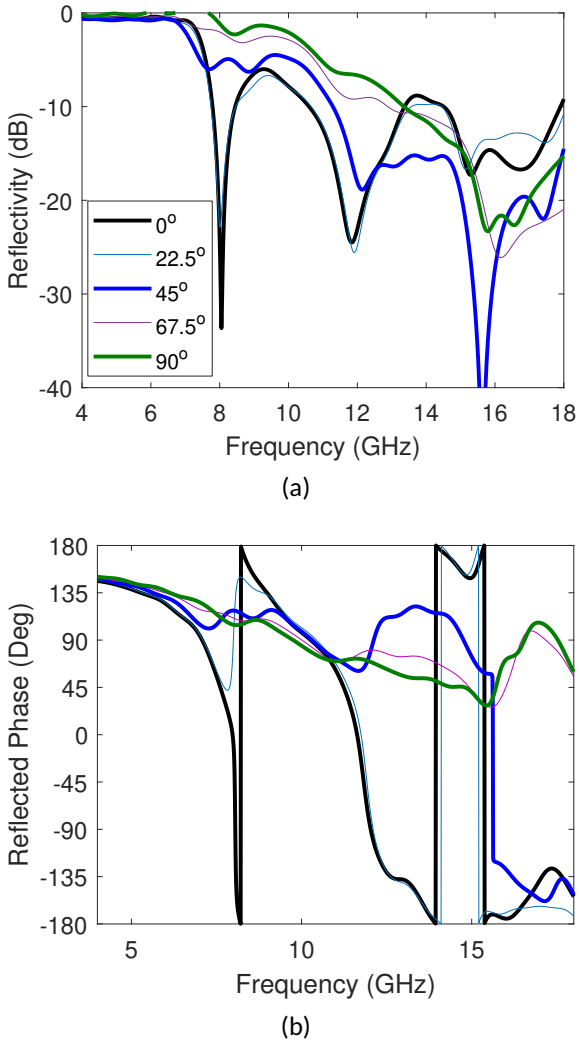

Figure 10: Measured reflection of HIS at various different rotation angles, (a) Magnitude, (b) Phase

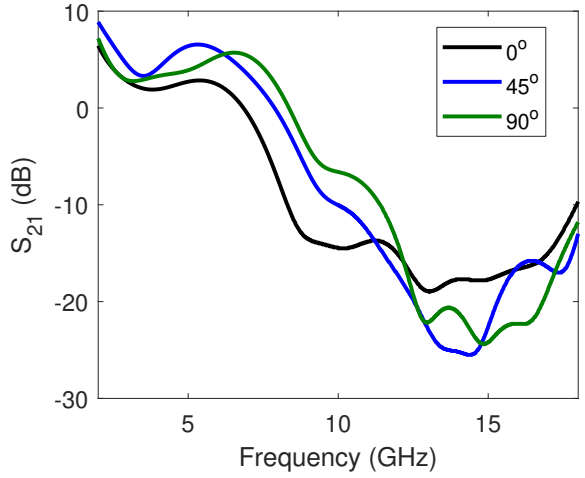

Figure 11: Measured surface wave suppression at different rotation angles

7 CONCLUSIONS

A fully knitted HIS co-designed for reduced knitting time and good electromagnetic performance has been presented, allowing broadband operation with 20 times shorter production times. In the ideal orientation,

with the incident E-field aligned with the wale of the conductive fabric, there is greater than 10 dB suppression of surface waves between 8 GHz and 18 GHz. However, this reduces to 12 GHz through 18 GHz when in the least advantageous orientation, where the E-field aligns with the course of the fabric. In-depth modeling of the structure has given insights into how knitted metasurfaces should be designed, separating the impact of the macro- and micro-structures created by the manufacturing process. An isotropic model was able to predict the main resonances, though not the polarized nature of the surface, while an anisotropic model was able to predict the polarized behavior at the fundamental resonance, but not at higher frequencies. Future work will combine this modeling approach with manufacturing to co-design structures with more predictable performance, and explore different knitting techniques to reduce anisotropy in the electromagnetic response.

References

Ali, U., Ullah, S., Basir, A., Kamal, B., Matekovits, L., and Yoo, H. (2023). Design and sar analysis of amc-based fabric antenna for body-centric communication. *IEEE Access*, 11:73894–73911, DOI: 10.1109/ACCESS.2023.3295993.

Ashyap, A. Y. I., Dahlan, S. H. B., Abidin, Z. Z., Rahim, S. K. A., Majid, H. A., Alqadami, A. S. M., and Atrash, M. E. (2021a). Fully fabric high impedance surface-enabled antenna for wearable medical applications. *IEEE Access*, 9:6948–6960, DOI: 10.1109/ACCESS.2021.3049491.

Ashyap, A. Y. I., Elamin, N. I. M., Dahlan, S. H., Abidin, Z. Z., See, C. H., Majid, H. A., AL-Fadhali, N., Mukred, J. A. A., Saleh, G., and Esmail, B. A. F. (2021b). Via-less electromagnetic band-gap-enabled antenna based on textile material for wearable applications. *PLOS ONE*, 16(1):1–21, DOI: 10.1371/journal.pone.0246057, https://doi.org/10.1371/journal.pone.0246057.

Baum, T. C., Ziolkowski, R. W., Ghorbani, K., and Nicholson, K. J. (2016). Embroidered active microwave composite preimpregnated electronics—pregtronics. *IEEE Transactions on Microwave Theory and Techniques*, 64(10):3175–3186, DOI: 10.1109/TMTT.2016.2600369.

Cerveny, M., Tennant, A., and Ford, K. L. (2023). An experimental system for the measurement of electromagnetic propagation on curved surfaces. In *2023 17th European Conference on Antennas and Propagation (EuCAP)*, pages 1–4. DOI: 10.23919/EuCAP57121.2023.10133035.

Ferreira, D., Caldeirinha, R. F., Cuinas, I., and Fernandes, T. R. (2018). A review of manufacturing materials and production methods for frequency-selective structures [wireless corner]. *IEEE Antennas and Propagation Magazine*, 60(6):110–119, DOI: 10.1109/MAP.2018.2870583.

Karger-Kocsis, J., Czigány, T., Gaál, J., and Ostgathe, M. (1996). Stiffness and strength anisotropy in the tensile response of weft knitted fabric-reinforced peek- and pet-composites. *Advanced Composites Letters*, 5(3):096369359600500301, DOI: 10.1177/096369359600500301, https://doi.org/10.1177/096369359600500301.

Keshwani, V. R. and Rathod, S. S. (2022). Dual band ebg with low sar for wearable applications. In *2022 IEEE Microwaves, Antennas, and Propagation Conference (MAPCON)*, pages 1484–1489. DOI: 10.1109/MAPCON56011.2022.10046951.

Liu, Y., Li, W., and Zhao, X. (2019). Influence of the yarn fineness and stitch length of polyester knitted fabric on the dielectric constant. *Fibres & Textiles in Eastern Europe*.

Salonen, P., Yang, F., Rahmat-Samii, Y., and Kivikoski, M. (2004). Webga - wearable electromagnetic band-gap antenna. In *IEEE Antennas and Propagation Society Symposium, 2004.*, volume 1, pages 451–454 Vol.1. DOI: 10.1109/APS.2004.1329671.

Seager, R., Chauraya, A., Bowman, J., Broughton, M., Philpott, R., and Nimkulrat, N. (2013). Fabric based frequency selective surfaces using weaving and screen printing. *Electronics Letters*, 49(24):1507–1509, DOI: https://doi.org/10.1049/el.2013.2314, https://ietresearch.onlinelibrary.wiley.com/doi/abs/10.1049/el.2013.2314.

Shamsuri Agus, A. N. S., Sabapathy, T., Jusoh, M., Abdelghany, M. A., Hossain, K., Padmanathan, S., Al-Bawri, S. S., and Soh, P. J. (2022). Combined ris and ebg surfaces inspired meta-wearable textile mimo antenna using viscose-wool felt. *Polymers*, 14(10), ISSN: 2073-4360, DOI: 10.3390/polym14101989, https://www.mdpi.com/2073-4360/14/10/1989.

Sievenpiper, D. F. (1999). *High-impedance electromagnetic surfaces*. University of California, Los Angeles.

Tennant, A., Hurley, W., and Dias, T. (2013). Knitted, textile, high impedance surface with integrated conducting vias. *Electronics Letters*, 49(1):8–10, DOI: https://doi.org/10.1049/el.2012.3896, https://ietresearch.onlinelibrary.wiley.com/doi/abs/10.1049/el.2012.3896.

Wajid, A., Ahmad, A., Ullah, S., Choi, D.-y., and Islam, F. U. (2022). Performance analysis of wearable dual-band patch antenna based on ebg and srr surfaces. *Sensors*, 22(14), ISSN: 1424-8220, DOI: 10.3390/s22145208, https://www.mdpi.com/1424-8220/22/14/5208.

Whittow, W., Li, Y., Torah, R., Yang, K., Beeby, S., and Tudor, J. (2014). Printed frequency selective surfaces on textiles. *Electronics Letters*, 50(13):916–917, DOI: https://doi.org/10.1049/el.2014.0955, https://ietresearch.onlinelibrary.wiley.com/doi/abs/10.1049/el.2014.0955.